A Distributed and Robust Energy Management System for Networked Hybrid AC/DC Microgrids

Xu, Qianwen; Zhao, Tianyang; Xu, Yan; Xu, Zhao Z.; Wang, Peng; Blaabjerg, Frede

Published in:
I E E E Transactions on Smart Grid

DOI (link to publication from Publisher):
10.1109/TSG.2019.2961737

Publication date:
2020

Document Version
Accepted author manuscript, peer reviewed version

This article has been accepted for publication in a future issue of this journal, but has not been fully edited. Content may change prior to final publication. Citation information: DOI 10.1109/TSG.2019.2961737, IEEE Transactions on Smart Grid

A Distributed and Robust Energy Management System for Networked Hybrid AC/DC Microgrids

Qianwen Xu, *Member, IEEE,* Tianyang Zhao, *Member, IEEE,* Yan Xu, *Member, IEEE,* Zhao Xu, *Senior Member, IEEE,* Peng Wang, *Fellow, IEEE,* and Frede Blaabjerg, *Fellow, IEEE*

***Abstract*—Hybrid AC/DC microgrids (MGs) provide efficient integration of renewable sources into grids and the interconnection of multiple MGs can improve system reliability, efficiency and economy by energy sharing. In this paper, a distributed and robust energy management system is proposed for networked hybrid AC/DC MGs. For each individual MG, an adjustable robust optimization model is proposed to optimize its individual operational cost considering the uncertainty of the renewable generation and load demand. For the networked-MGs system, the energy sharing information of each MG is coordinated by the DC network to minimize the power transmission loss with network constraints. The overall optimization model is formulated, exactly convexified and solved in a distributed manner by the alternating direction method of multipliers (ADMM), where only limited information is required from each MG entity (i.e., the power injection to the network) and thus information privacy is guaranteed. Simulations of the networked hybrid AC/DC MGs are conducted to demonstrate the effectiveness of the proposed energy management system.**

***Index Terms*—hybrid AC/DC microgrid, networked microgrids, energy management, uncertainty, distributed**

I. Introduction

MICROGRID (MG), which integrates a group of distributed generators, energy storage systems (ESSs) and local loads, provides a building block of smart grid [1], [2]. In recent years, hybrid AC/DC MGs are proposed and attract much attention [3], [4]. Hybrid AC/DC MGs reduce multiple power conversion stages in individual AC or DC MGs, and provide efficient integration of various renewable AC or DC sources to the utility grid [5], [6]. To further enhance system reliability, efficiency and economy, energy sharing among networked multiple MGs becomes a promising solution. To achieve optimal performance of the networked MGs, i.e., to optimize the energy cooperation among MGs and energy scheduling within each MG (e.g., the energy generation of DGs, charge/discharge of ESSs), an energy management system (EMS) is significantly important.

Manuscript received Feb 13, 2019; revised Aug 7 and Nov 1, 2019; accepted Dec 19, 2019. This work was supported in part by Ministry of Education (MOE), Republic of Singapore, under grant AcRF TIER 1 2019-T1-001-069 (RG75/19), in part by National Research Foundation (NRF) of Singapore under project NRF2018-SR2001-018, in part by National Natural Science Foundation of China (Grant No. 71971183&71931003) and in part by Wallenberg-NTU Presidential Postdoc Fellowship in Nanyang Technological University, Singapore. Y. Xu's work is supported by Nanyang Assistant Professorship from Nanyang Technological University, Singapore.

Q. Xu, Y. Xu and P. Wang are with the school of Electrical and Electronic Engineering, Nanyang Technological University, Singapore, e-mail: qxu007@e.ntu.edu.sg, xuyan@ntu.edu.sg,epwang@ntu.edu.sg

T. Zhao is with the energy research institutes, Nanyang Technological University, Singapore, e-mail: zhaoty@ntu.edu.sg

Z. Xu is with both Shenzhen Research Institute and Department of Electrical Engineering, The Hong Kong Polytechnic University, Hung Hom, Hong Kong and he is also with Changsha University of Science and Technology, e-mail: eezhaoxu@polyu.edu.hk.

F. Blaabjerg is with the Department of Energy Technology, Aalborg University, Denmark, e-mail: fbl@et.aau.dk

Many related works have been proposed for energy sharing among interconnected AC MGs. A coordinated control algorithm is presented in [7] for a distribution management system by considering the distribution network as coupled MGs. In [8], a joint energy trading and scheduling strategy is designed for interconnected MGs band based on Nash bargaining theory and a distributed algorithm is developed to solve the optimization problem. A two-level EMS is proposed in [9] for a MG community based on hierarchical optimization. The lower level optimizes the power output of individual MGs and the higher level determines power exchanges among MGs. However, in the above works, the renewable generations are assumed to be perfectly forecast and uncertainties are not considered.

Several research works have developed EMSs for multiple MGs considering uncertainties. Ref [10] introduces a hierarchical bi-level EMS framework for the utility and multiple coupled MGs and Taguchi's orthogonal array testing algorithm is utilized to represent the uncertainties of renewable generations and load. Ref [11] proposes a distributed robust optimal scheduling algorithm to optimize the total operational cost of multiple MGs in the real-time energy market. The uncertainties are handed using an adjustable robust optimization technique. However, these works only consider aggregated power balance while omitting the underlying power distribution network and the associated power flow constraints [10], [11].

Power flow and system operational constraints are taken into consideration in some recent works. The study in [12] develops a two-level optimization model for coordination energy management between distribution systems and clustered MGs with a power reserve mechanism and a game theory-based strategy. But it does not consider uncertainties in the forecast information. In [13], the energy management of networked MGs are solved as a stochastic bi-level problem with the distribution network operator in the upper level and individual MGs in the lower level. Uncertainties of renewable generations and loads are managed by the two-stage stochastic optimization. However, in this work, uncertainties in each MG will impact the power flow on the distribution network, indicating the scheme is semi-distributed. Moreover, in the stochastic optimization formulation, the probability distribution functions of the uncertainties are required.

Noted that all the above works [7]- [13] are for energy

This article has been accepted for publication in a future issue of this journal, but has not been fully edited. Content may change prior to final publication. Citation information: DOI 10.1109/TSG.2019.2961737, IEEE Transactions on Smart Grid

management with multiple AC MGs. Considering different features of hybrid AC/DC MGs, e.g., the existence of bidirectional interlinking converters and the requirements for power balance in both subgrids (AC and DC), research gaps still exist for the energy management of networked hybrid AC/DC MGs. Considering different features of hybrid AC/DC MGs, e.g., the existence of bidirectional interlinking converters and the requirements for power balance in both subgrids (AC and DC), energy management of hybrid AC/DC MGs are different from that of AC MGs. There are several works about energy management of hybrid AC/DC MGs. Ref. [14] proposes a real time ems for a residential hybrid AC/DC MG, which performs an 24 hour ahead optimization to schedule charge/discharge of ESS and energy consumption from the grid; but the uncertainties in RES generation and building loads are not considered. In [15], an up-down operation model is proposed where a day-ahead economic operation model is constructed considering interconnection of AC and DC subgrids in the system level, and a real time controller for battery and inverter is proposed in the device level; the uncertainties are considered by two-stage stochastic optimization. Ref. [16] proposes an energy management system for hybrid AC/DC MGs with the uncertainties modeled by a stochastic framework based on an unscented transform; crow search algorithm is proposed to solve the optimization problem. Ref. [17] proposes a probabilistic economic dispatch tool for energy management of hybrid AC/DC MGs considering uncertainties. However, in these works [14]–[17], the uncertainties are either not considered, or modeled by stochastic optimization formulation, which requires the probability distribution functions of the uncertainties. Moreover, these works only consider single hybrid AC/DC MG, it is necessary to investigate the energy management of networked hybrid AC/DC MGs.

For the energy management of networked hybrid AC/DC MGs, there are some factors that should be taken care of, including the uncertainty management and network power flow constraints. Moreover, in real situations, MGs are managed by different entities. They are unwilling to share their key information, e.g., types, characteristics, capacities of energy sources and loads, to others for the sake of privacy. Therefore, a distributed energy management system (EMS) considering the above factors should be developed for the coordination of networked hybrid AC/DC MGs.

This paper proposes a robust and distributed EMS for networked hybrid AC/DC MGs. The hybrid AC/DC MGs are interconnected through a DC network. For each single MG, an adjustable robust optimization model is proposed to minimize its operational cost considering the uncertainties of renewable generation and loads by scheduling power outputs and participation factors of the utility grid (UG), DGs and ESSs. No probability distribution functions are required. For the overall networked-MGs system, the energy sharing information of each MG is coordinated through the DC network to minimize the power transmission loss, and the corresponding optimization model is formulated, convexified and solved in a distributed manner by the alternating direction method of multipliers (ADMM). Within this EMS, each MG acts as an independent agent to determine its own operational schedule with only boundary information to be exchanged with the DC network. The major contributions of this paper are summarized as follows:

1) An energy management system is developed for the networked hybrid AC/DC MGs to optimize the operational costs of individual MGs and power transmission loss of the network. The nonconvexities caused by the bidirectional power flow in the hybrid AC/DC MG and the DC network are relaxed exatcly.

2) The proposed EMS is robust against the uncertainties of renewable generations and loads.

3) The proposed EMS is distributed with the protected information privacy of each MG entity.

This paper is organized as follows: Section II describes the architecture of the networked hybrid AC/DC MGs and the proposed EMS. Section III presents the formulation of the optimization problem for the networked MGs. Section IV proposes a robust optimization model for the single MG to address the uncertainties. Section V develops the distributed solution for the networked MGs. Case studies are performed with simulation analysis in Section VI. Conclusions are drawn in Section VII.

II. Distributed Energy Management of Networked Hybrid AC/DC MGs

Fig. 1 illustrates the architecture of networked hybrid AC/DC MGs. For a single hybrid AC/DC MG, various sources and loads are connected to AC and DC sub-grids appropriately. In AC sub-grid, diesel generators (DGs) and AC loads are connected to the common AC bus; In DC sub-grid, photovoltaics (PV), energy storage systems (ESSs) and DC loads are connected to the common DC bus. AC sub-grid and DC subgrid are tied by bidirectional interlinking converters (BICs). The utility grid (UG) is interfaced to the AC bus. The networked MGs are formed by interconnecting multiple MGs through a DC network at their respective DC buses. It is noted that the DC network can be modified based on the interconnection relationship of multiple MGs, and can also be extended for large-scale system applications. The development of this architecture is because of the following reasons:

1) Hybrid AC/DC MGs inherit the advantages of AC MGs and DC MGs: they reduce multiple power conversion stages for the integration of various sources and loads; and are compatible to the conventional utility grid [3]-[6].

2) DC network allows easier power merging and simpler system analysis (no issues of reactive power sharing, frequency synchronization, etc.) [18].

3) Networked multiple microgrids have enhanced system reliability, efficiency and economy compared with individual microgrids by energy sharing through the network.

This paper proposes a distributed and robust EMS for the networked-MGs system. For an individual MG, it has its own objective to minimize its operational cost subject to power balance constraints at the AC sub-grid and DC sub-grid, as well as power and energy capacity constraints of the UG, DGs, ESSs and BICs. Considering uncertainties of renewable generation and load demand, an adjustable robust model is proposed to minimize the operational costs of individual MGs

This article has been accepted for publication in a future issue of this journal, but has not been fully edited. Content may change prior to final publication. Citation information: DOI 10.1109/TSG.2019.2961737, IEEE Transactions on Smart Grid

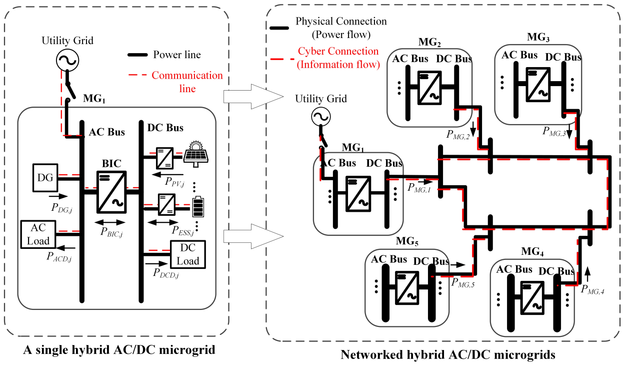

Fig. 1. The architecture of networked hybrid AC/DC microgrids

by scheduling the power outputs of the UG, DGs, ESSs, BICs and MGs, and participation factors of the UG, DGs and ESSs. For the networked MGs, MGs with energy surplus will supply energy to the DC network and MGs with energy deficit will absorb energy from the DC network; the energy sharing among MGs is scheduled through the DC network to minimize the power transmission loss with the network limitations. Then the overall optimization model of the networked-MGs system is formulated to minimize operational costs of the MGs and the power transmission loss. As MGs are often owned by different entities, they are unwilling to share the detailed information with others (such as dispatched power output of DGs and ESSs, etc.). To ensure the information privacy and computational efficiency, the optimization model is solved by a distributed algorithm based on ADMM with limited information exchange (i.e. the power injection to the network). The mathematical optimization model and solution algorithms for the proposed EMS is described in Section III, IV and V in detail.

III. Mathematical Formulation

This section provides individual optimization model for the single hybrid AC/DC MG and the coordinated operation model for the networked-MGs system. Considering the specific operational time scale, these models are formulated as intra-day dynamic optimal power flow (OPF) models, i.e., the energy scheduling within the coming hours are considered. The time horizon, denoted by $\mathcal{T}$, is divided into equal time steps, i.e., Δt.

A. A Single Hybrid AC/DC Microgrid

For MG i, its objective is to minimize the operational cost along the time horizon $\mathcal{T}$. Its optimization problem is formulated as follows.

$$\begin{aligned}\min_{\mathbf{p}_i(t),\forall t\in\mathcal{T}} & \sum_{t\in\mathcal{T}} f(\mathbf{p}_i(t)) = \\ \sum_{t\in\mathcal{T}} & [\underbrace{a_{\text{DG},0,i}p_{\text{DG},i}(t)^2 + a_{\text{DG},1,i}p_{\text{DG},i}(t) + a_{\text{DG},2,i}}_{\text{Fuel cost of DG}} + \\ & + \underbrace{b_{\text{PV},i}p_{\text{PV},i}(t)}_{\text{Operation cost of PV}} + \underbrace{\lambda(t)p_{\text{UG},i}(t)}_{\text{Electricity cost}} \\ & + \underbrace{c_{\text{ESS,dc},i}p_{\text{ESS,dc},i}(t) + c_{\text{ESS,c},i}p_{\text{ESS,c},i}(t)}_{\text{Operation cost of ESS}}]\Delta t\end{aligned} \tag{1}$$

s.t.

a) Power balance

$$\begin{aligned}p_{\text{UG},i}(t) + p_{\text{DG},i}(t) + \eta_{\text{D2A},i}p_{\text{D2A},i}(t) = \\ p_{\text{AC},i}(t) + p_{\text{A2D},i}(t), \forall t\in\mathcal{T}\end{aligned} \tag{2}$$

$$\begin{aligned}p_{\text{ESS,dc},i}(t) - p_{\text{ESS,c},i}(t) + \eta_{\text{A2D},i}p_{\text{A2D},i}(t) + p_{\text{PV},i}(t) \\ = p_{\text{DC},i}(t) + p_{\text{D2A},i}(t) + p_{\text{MG},i}(t), \forall t\in\mathcal{T}\end{aligned} \tag{3}$$

b) Energy storage capacity balance

$$\begin{aligned}E_{\text{ESS},i}(t) = E_{\text{ESS},i}(t-\Delta t) + p_{\text{ESS,c},i}(t)\eta_{\text{ESS,c},i}\Delta t - \\ \frac{p_{\text{ESS,dc},i}(t)\Delta t}{\eta_{\text{ESS,dc},i}}, \forall t\in\mathcal{T}\end{aligned} \tag{4}$$

c) Power, ramp rate and capacity constraints

$$P_{\text{DG,min},i} \le p_{\text{DG},i}(t) \le P_{\text{DG,max},i}, \forall t\in\mathcal{T} \tag{5}$$

$$\begin{aligned}-R_{\text{DG,down},i} \le p_{\text{DG},i}(t) - p_{\text{DG},i}(t-\Delta t) \\ \le R_{\text{DG,up},i}, \forall t\in\mathcal{T}\end{aligned} \tag{6}$$

$$0 \le p_{\text{ESS,dc},i}(t) \le P_{\text{ESS,dc,max},i}, \forall t\in\mathcal{T} \tag{7}$$

$$0 \le p_{\text{ESS,c},i}(t) \le P_{\text{ESS,c,max},i}, \forall t\in\mathcal{T} \tag{8}$$

$$E_{\text{ESS,min},i} \le E_{\text{ESS},i}(t) \le E_{\text{ESS,max},i}, \forall t\in\mathcal{T} \tag{9}$$

$$0 \le p_{\text{UG},i}(t) \le P_{\text{UG,max},i}, \forall t\in\mathcal{T} \tag{10}$$

$$0 \le p_{\text{A2D},i}(t) \le P_{\text{BIC,max},i}, \forall t\in\mathcal{T} \tag{11}$$

$$0 \le p_{\text{D2A},i}(t) \le P_{\text{BIC,max},i}, \forall t\in\mathcal{T} \tag{12}$$

d) Bi-directional power flow constraints

$$p_{\text{ESS,dc},i}(t)p_{\text{ESS,c},i}(t) = 0, \forall t\in\mathcal{T} \tag{13}$$

$$p_{\text{D2A},i}(t)p_{\text{A2D},i}(t) = 0, \forall t\in\mathcal{T} \tag{14}$$

where $\mathbf{p}_i(t) := \{p_{\text{UG},i}(t), p_{\text{DG},i}(t), p_{\text{ESS,c},i}(t), p_{\text{ESS,dc},i}(t), p_{\text{MG},i}(t), p_{\text{D2A},i}(t), p_{\text{A2D},i}(t)\}$. $p_{\text{UG},i}(t)$, $p_{\text{DG},i}(t)$, $p_{\text{ESS,c},i}(t)$, $p_{\text{ESS,dc},i}(t)$, $p_{\text{PV},i}(t)$ and $p_{\text{MG},i}(t)$ are real power output of UG, DG, ESS (charge and discharge), PV and power exchange between the i-th MG and the network during time slot t, respectively. $p_{\text{A2D},i}(t)$ and $p_{\text{D2A},i}(t)$ are energy transferring from AC bus to DC bus and from DC bus to AC bus through BIC with efficiency $\eta_{\text{A2D},i}$ and $\eta_{\text{D2A},i}$ in the i-th MG, during time slot t, respectively. $p_{\text{AC},i}(t)$, $p_{\text{DC},i}(t)$ and $p_{\text{PV},i}(t)$ are real AC load, DC load and PV output within the i-th MG during time slot t, respectively. $\eta_{\text{ESS,c},i}$ and $\eta_{\text{ESS,dc},i}$ are the charging and discharging efficiency of ESS in the i-th MG, respectively. $a_{\text{DG},0,i}$, $a_{\text{DG},1,i}$, $a_{\text{DG},2,i}$, $b_{\text{PV},i}$, $c_{\text{ESS,dc},i}$ and $c_{\text{ESS,c},i}$ are the cost parameter of DG, PV and ESS in the i-th MG, respectively.

$b_{\text{PV},i}$ represents for the operational cost of PV system, using levelized cost of energy (LCOE) model [18]–[20]. $c_{\text{ESS,dc},i}$ and $c_{\text{ESS,c},i}$ are to represent the operational cost of ESS [19], using LCOE model [21]. $\lambda(t)$ is the electricity tariff during time slot t. $P_{\text{DG,min},i}$ and $P_{\text{DG,max},i}$ are the minimal and maximal output of DG within the i-th MG, respectively. $R_{\text{DG,down},i}$ and $R_{\text{DG,up},i}$ are the ramp down and ramp up rate of DG in the i-th MG, respectively. $P_{\text{ESS,c,max},i}$ and $P_{\text{ESS,dc,max},i}$ are the maximal charging and discharging rate of ESS in the i-th MG, respectively. $E_{\text{ESS,max},i}$ and $E_{\text{ESS,min},i}$ are the maximal and minimal eneregy status of ESS in the i-th MG, respectively. $P_{\text{UG,max},i}$ is the maximal power exchange between UG and MG i. $P_{\text{BIC,max},i}$ is the maximal real power converted on BIC in the i-th MG.

Eq. (1) includes the operational cost of DGs, PVs, ESSs, and cost charged by the UG. Eq. (2) and Eq. (3) show power balance at AC bus and DC bus in the i-th MG, respectively. The energy status change of ESS with respect to the charging and discharging is shown in Eq.(4). Power capacity and ramp rate limitation of DG i are shown in Eq.(5) and Eq.(6), respectively. The charging and discharging rate limitations of ESS are shown in Eq.(7) and Eq.(8), respectively. The energy status of ESS is limited by Eq.(9). The limitation of power exchange between the MG i and utility grid is depicted by Eq.(10). The limitations of power transferring from AC to DC and DC to AC are illustrated by Eq.(11) and Eq.(12), respectively. The complementary characteristics of the bi-directional power flow constrains on BIC and ESS are depicted by Eq.(13) and Eq.(14), respectively.

Lemma 1: Constraints (13)-(14) can be omitted in problem (1)-(14), provided that

- $a_{\text{DG},0,i} > 0$, $c_{\text{ESS,dc},i} > 0$ and $c_{\text{ESS,c},i} > 0$.

The lemma is proved in Appendix A.

Remarks: The LCOE model is adopted in this paper to make different energy sources comparative, e.g., batteries, solar PV and diesel generators. The LCOE means levelized cost of energy, which represents the average revenue per unit of electricity generated that would be required to recover the costs of building and operating a generating plant during an assumed financial life and duty cycle [18]. LCOE is different from the marginal cost, as it is the sum of levelized capital cost, levelized fixed O&M, levelized variable O&M and levelized transmission cost. The LCOE cost of solar PV, wind power, hydropower and many other sources are analysed in [18]. Regarding solar PV, its fixed cost is high and variable cost is negligible. For batteries, its operation cost model is still an ongoing research, especially considering the degradation, safety and etc, and LCOE model of batteries has been applied in operational problems [18-21].

B. Networked Microgrids

The networked-MGs system is formed by interconnecting multiple hybrid AC/DC MGs through a DC network. The energy sharing among MGs is realized using this DC network, and the power flow constraints on the DC network should be considered. The DC network is denoted by a connected network $\mathcal{G}$:=$(\mathcal{N},\mathcal{E})$, where $\mathcal{N}$ is the set of buses connected with MGs, $\mathcal{E}$ is the set of transmission lines connecting the MGs. The branch power flow model [22] is adopted to depict the power flows on $\mathcal{G}$, as follows.

$$\sum_{k:k\to j} P_{jk}(t) = \sum_{i:i\to j} (P_{ij}(t) - r_{ij}l_{ij}(t)) + p_{\text{MG},j}(t), \quad \forall j \in \mathcal{N}, t \in \mathcal{T} \tag{15}$$

$$v_j(t) - v_k(t) = 2r_{jk}P_{jk}(t) - r_{jk}^2 l_{jk}(t), \forall j \to k \in \mathcal{E}, t \in \mathcal{T} \tag{16}$$

$$v_j(t) l_{jk}(t) = P_{jk}^2(t), \forall j \to k \in \mathcal{E}, t \in \mathcal{T} \tag{17}$$

where $P_{jk}(t)$ is the active power on line $j \to k$, r_{jk} is the resistance of line $j \to k$, $l_{jk}(t) := I_{jk}^2(t)$, $I_{jk}(t)$ is the current on line $j \to k$, $v_j(t) := V_j^2(t)$, $V_j(t)$ is the voltage magnitude of bus j.

The DC network coordinates the energy sharing of MGs to minimize the real power losses on the DC network. Then the overall objective function for the networked-MGs system is to minimize the operational costs of individual MGs and the real power losses on the DC network. The optimization model is shown as follows.

$$\begin{aligned} \min_{\substack{\mathbf{p}_j(t),\\ P_{jk}(t), l_{jk}(t), v_j(t)\\ \forall j\in\mathcal{N}, j\to k\in\mathcal{E}, t\in\mathcal{T}}} \quad & \mathbb{E}\sum_{t\in\mathcal{T}} \{ f(\mathbf{p}_i(t)) + \sum_{j:j\to k} l_{jk}(t) r_{jk} \} \\ \text{s.t.} \quad & \\ & (2)-(12), (15)-(17) \\ & v_{j,\text{min}} \le v_j(t) \le v_{j,\text{max}}, \forall j \in \mathcal{N}, t \in \mathcal{T} \\ & 0 \le l_{jk}(t) \le l_{jk,\text{max}}, \forall j \to k \in \mathcal{E}, t \in \mathcal{T} \end{aligned} \tag{18}$$

where $v_{j,\text{min}}$ and $v_{j,\text{max}}$ are the minimal and maximal limitations on the voltage magnitude of bus j. $l_{jk,\text{max}}$ is the thermal current limitation on line $j \to k$.

This model shows that MGs can share energy with other MGs through the DC network, while satisfying the technical limitations on the voltage magnitude and line flows. Together with the uncertainty modelling in section IV.A and affine policy in section IV.B, problem (18) will be formulated as a robust optimization problem.

IV. Adjustable Robust Optimization for the Single Microgrid

For a single MG with the optimization model described by (1)-(12), the variables $p_{\text{PV},i}(t)$, $p_{\text{AC},i}(t)$ and $p_{\text{DC},i}(t)$ are the real power output of PV, AC load and DC load. Due to the stochastic nature of renewable generation and uncertainty of loads, the forecast information might not perfectly follow real-time values during operation. In this section, an adjustable robust optimization model is proposed to handle the uncertainties of RESs and load in individual MGs.

A. Uncertainty Modeling

The variations of PV, AC load, and DC load are considered and denoted as $\xi_{\text{PV},i}(t)$, $\xi_{\text{AC},i}(t)$ and $\xi_{\text{DC},i}(t)$, respectively. Unlike stochastic approaches which need an accurate specification of the probability density function (PDF) of the uncertain parameters, the robust optimization only requires knowledge of the range of the variations of the uncertain

This article has been accepted for publication in a future issue of this journal, but has not been fully edited. Content may change prior to final publication. Citation information: DOI 10.1109/TSG.2019.2961737, IEEE Transactions on Smart Grid

parameters. The variations of real values from the forecast data are depicted by the following zero-mean uncertainty sets:

$$P_{\text{PV},i}(t) - p_{\text{PV},i}(t) = \xi_{\text{PV},i}(t) \in \quad [-\xi^{\max}_{\text{PV},i}, \xi^{\max}_{\text{PV},i}] \tag{19}$$

$$P_{\text{AC},i}(t) - p_{\text{AC},i}(t) = \xi_{\text{AC},i}(t) \in \quad [-\xi^{\max}_{\text{AC},i}, \xi^{\max}_{\text{AC},i}] \tag{20}$$

$$P_{\text{DC},i}(t) - p_{\text{DC},i}(t) = \xi_{\text{DC},i}(t) \in \quad [-\xi^{\max}_{\text{DC},i}, \xi^{\max}_{\text{DC},i}] \tag{21}$$

where $P_{\text{PV},i}(t)$, $P_{\text{AC},i}(t)$ and $P_{\text{DC},i}(t)$ are forecast value of PV output, AC load and DC load. These intervals can be obtained using mean variance estimation approaches [23], where a neural network forecasts the mean and the other variance of normal distributions. The forecast error intervals can be obtained under given confidential level.

Without considering the correlation among loads and PV output, the aggregated forecast error, i.e., $\xi_i(t)$, can be expressed as

$$\begin{aligned} &\xi_i(t) = \xi_{\text{AC},i}(t) + \xi_{\text{DC},i}(t) - \xi_{\text{PV},i}(t) \in \\ &[-\xi^{\max}_{\text{AC},i} - \xi^{\max}_{\text{DC},i} - \xi^{\max}_{\text{PV},i}, \xi^{\max}_{\text{AC},i} + \xi^{\max}_{\text{DC},i} + \xi^{\max}_{\text{PV},i}] \end{aligned} \tag{22}$$

B. Affinely Adjustable Robust Modeling

As the lumped uncertainty $\xi_i(t)$ always fluctuates within each scheduling period, the affinely adjustable robust optimization method is adopted to address the uncertainties and maintain the power balance within the individual MGs [24]. It consists of two parts. First, the base-point generation values of the UG, DG and ESS are acquired from the energy scheduling result according to the forecast information without the uncertainties; then the participation factors are employed to adjust the power generation around the base-point values to compensate the uncertainties (i.e. forecast error $\xi_i(t)$). As such, the real-time power output of the UG, DG and ESS can be described by the following affine policies with the corresponding participation factors:

$$p_{\text{UG},i}(t) = P_{\text{UG},i}(t) - \beta_{\text{UG},i}(t)\xi_i(t), \forall t \in \mathcal{T} \tag{23}$$

$$p_{\text{DG},i}(t) = P_{\text{DG},i}(t) - \beta_{\text{DG},i}(t)\xi_i(t), \forall t \in \mathcal{T} \tag{24}$$

$$p_{\text{ESS},i}(t) = P_{\text{ESS,dc},i}(t) - P_{\text{ESS,c},i}(t) - \beta_{\text{ESS},i}(t)\xi_i(t), \forall t \in \mathcal{T} \tag{25}$$

where $P_{\text{UG},i}(t)$, $P_{\text{DG},i}(t)$, $P_{\text{ESS,dc},i}(t)$ and $P_{\text{ESS,c},i}(t)$ are the base-point values of the UG, DG and ESS (in discharging and charging modes) within the i-th MG during time slot t, respectively. $\beta_{\text{UG},i}(t)$,$\beta_{\text{DG},i}(t)$ and $\beta_{\text{ESS},i}(t)$ are the participation factors of the UG, DG and ESS during time slot t, respectively.

Based on power balance conditions in Eq.(2)-Eq.(3), the following condition can be obtained without considering the power losses on BIC.

$$\beta_{\text{DG},i} + \beta_{\text{UG},i} + \beta_{\text{ESS},i} = 1, \forall t \in \mathcal{T} \tag{26}$$

C. Robust Optimization Modelling

According to the affinely adjustable robust modeling functions in (23)-(26), the robust optimization model for a single MG in (1)-(12) with the uncertainties can be reformulated to minimize the expected operational cost, given by

$$\begin{aligned} &\min_{\mathbf{P}_i(t),\beta_i(t),\forall t\in\mathcal{T}} \mathbb{E}\sum_{t\in\mathcal{T}} f(\mathbf{P}_i(t), \beta_i(t)) = \\ &\sum_{t\in\mathcal{T}} [a_{\text{DG},0,i}P^2_{\text{DG},i}(t) + a_{\text{DG},1,i}P_{\text{DG},i}(t) + a_{\text{DG},2,i} + \\ &a_{\text{DG},0,i}\beta^2_{\text{DG},i}(t) + b_{\text{PV},i}P_{\text{PV},i}(t) + \lambda(t)P_{\text{UG},i}(t) + \\ &c_{\text{ESS,dc},i}P_{\text{ESS,dc},i}(t) + c_{\text{ESS,c},i}P_{\text{ESS,c},i}(t)]\Delta t \\ &\text{s.t.} \\ &\text{reformulated } (2) - (12) \text{ with base-point values } \mathbf{P}_i(t) \\ &\text{robust counterpart of Eq.}(5), (7), (8), (10) - (12) \end{aligned} \tag{27}$$

where $\mathbf{P}_i(t) := \{P_{\text{UG},i}(t), P_{\text{DG},i}(t), P_{\text{ESS,c},i}(t), P_{\text{ESS,dc},i}(t), P_{\text{MG},i}(t), P_{\text{D2A},i}(t), P_{\text{A2D},i}(t)\}, \quad t \in \mathcal{T}, \beta_i(t) := \{\beta_{\text{UG},i}(t), \beta_{\text{DG},i}(t), \beta_{\text{ESS},i}(t)\}, t \in \mathcal{T}$. $P_{\text{A2D},i}(t)$, $P_{\text{D2A},i}(t)$ and $P_{\text{MG},i}(t)$ are the base-point values of power converted from the AC bus to the DC bus, power converted from the DC bus to the AC bus and power exchange with the DC network in the i-th MG during time slot t. The base point values should also satisfy the constraints for real-time values in (2)-(12) by substituting the base-point values $\mathbf{P}_i(t)$ for real-time values $\mathbf{p}_i(t)$. Robust counterpart of constraints (5), (7) ,(8) and (10)-(12) are to guarantee the secure operation of DG, BIC and ESS, while adopting the affine policies in (23)-(26) and considering the uncertainties in (19)-(21), and the details formulation of the robust counterpart can be found in Appendix B. The detailed derivation of objective function in (27) is refered to Appendix A in [24].

Problem (27) is a non-convex quadratic programming problem. With this adjustable robust optimization model, uncertainties are managed locally within each MG and the power exchange of MG i with the DC network is controlled to follow the set-points $P_{\text{MG},i}(t)$.

V. Distributed Solution for Networked Microgrids

Based on the robust optimization model in Eq. (27), the optimization model for the overall networked-MGs system in Eq. (18) is reformulated as

$$\begin{aligned} &\min_{\substack{\mathbf{P}_j(t),\beta_j(t),\\ P_{jk}(t),l_{jk}(t),v_j(t)\\ \forall j\in\mathcal{N},j\to k\in\mathcal{E},t\in\mathcal{T}}} \mathbb{E}\sum_{t\in\mathcal{T}}\{f(\mathbf{P}_i(t), \beta_i(t)) + \sum_{j:j\to k} l_{jk}(t)r_{jk}\} \\ &\text{s.t.} \\ &\text{reformulated } (2) - (12) \text{ with base-point values } \mathbf{P}_i(t), \\ &\text{robust counterpart of Eq.}(5), (7), (8), (10) - (12) \\ &\text{Eq.}(15) - (17) \\ &v_{j,\min} \le v_j(t) \le v_{j,\max}, \forall j \in \mathcal{N}, t \in \mathcal{T} \\ &0 \le l_{jk}(t) \le l_{jk,\max}, \forall j \to k \in \mathcal{E}, t \in \mathcal{T} \end{aligned} \tag{28}$$

Due to the existence of non-convex constrain (17), problem (28) is a non-convex optimization problem, which might admit multiple local optima. Therefore, the convexification is performed first. Then a distributed algorithm is developed to solve the reformulated convex optimization problem.

A. Convexification

The constraint in (17) can be relaxed using the conic relaxation [25], shown as follows:

$$v_j(t)l_{jk}(t) \geq P_{jk}^2(t), \forall j \to k \in \mathcal{E}, t \in \mathcal{T} \tag{29}$$

After the reformulation, the non-convex problem (28) is reformulated to a convex quadratic constrained quadratic programming (QCQP) problem.

Lemma 2: Conic relaxation is exact for the following optimization problem.

$$\begin{aligned} &\min_{\substack{P_{\text{MG},j}(t),P_{jk}(t),l_{jk}(t),v_j(t)\\ \forall j\in\mathcal{N},j\to k\in\mathcal{E},t\in\mathcal{T}}} \sum_{t\in\mathcal{T}}\sum_{j:j\to k} l_{jk}(t)r_{jk}\\ &\text{s.t.}\\ &\text{Eq.}(15)-(17)\\ &v_{j,\text{min}} \leq v_j(t) \leq v_{\text{max}}, \forall j \in \mathcal{N}, t\in\mathcal{T}\\ &0 \leq l_{jk}(t) \leq l_{jk,\text{max}}, \forall j\to k \in \mathcal{E}, t\in\mathcal{T} \end{aligned} \tag{30}$$

where v_{max} is the upper voltage magnitude limitation for all buses. The lemma is proved in Appendix C.

Theorem 1: Conic relaxation (29) is exact for problem (30) provided that

- $a_{\text{DG},0,i} > 0$, $c_{\text{ESS,dc},i} > 0$ and $c_{\text{ESS,c},i} > 0$, $\forall i \in \mathcal{N}$.
- The upper voltage magnitude limitation for each bus is the same, i.e., $v_{j,\text{max}} = v_{\text{max}}, \forall j \in \mathcal{N}$.

The theorem is proved in Appendix D.

B. Distributed Solution

The problem in (28) is a centralized optimization problem. A centralized algorithm requires detailed models of each MG and the DC network, and it may suffer high computation burden and is rigid for system expansion. In order to design an efficient, scalable and private-preserving EMS, a distributed algorithm is developed using the auxiliary problem principle (APP) [26] and alternating direction method of multipliers (ADMM) [27].

First, APP is adopted to decompose the centralized optimization problem in (28) into sub-problems for a distributed implementation. Auxiliary variables, i.e., $\bar{P}_{\text{MG},i}(t), \forall i \in \mathcal{N}, t \in \mathcal{T}$, are introduced as duplication of $P_{\text{MG},i}(t), \forall i \in \mathcal{N}, t \in \mathcal{T}$. The auxiliary variables are optimized by the distribution operator, while the $\bar{P}_{\text{MG},i}(t), \forall t \in \mathcal{T}$ is optimized by each MG. In addition, the auxiliary variables should meet the following condition:

$$\bar{P}_{\text{MG},i}(t) = P_{\text{MG},i}(t), \forall i \in \mathcal{N}, t \in \mathcal{T} \tag{31}$$

With the introduction of auxiliary variables and constraints (31), the reformulated problem (28) remains a convex QCQP problem and can be solved distributively.

Next, ADMM is employed to solve the reformulated problem (28) in a distributed manner, as shown in algorithm 1. ADMM has advantages of easy distributed implementation, scalability and good convergence property compared to other distributed algorithms [27]. By using ADMM, each MG will solve its own optimization problem and transfer the scheduled energy exchange variables $P_{\text{MG},i}(t), \forall t \in \mathcal{T}$ to

Step 1: Initialization
$k = 0$
$y_i^k(t) = 0, P_{\text{MG},i}^k(t) = 0, \bar{P}_{\text{MG},i}^k(t) = 0, \forall i \in \mathcal{N}, t \in \mathcal{T}$
Step 2: Sub problem for each MG
$k = k + 1$
for $i \in \mathcal{N}$

$$\begin{aligned} \mathbf{P}_{\text{MG},i}^k = &\underset{\mathbf{p}_i(t),\beta_i(t),\forall t\in\mathcal{T}}{\text{argmin}} \{\mathbb{E}\sum_{t\in\mathcal{T}} f(\mathbf{p}_i(t),\beta_i(t))\\ &- y_i^k(t)P_{\text{MG},i}^k(t) + \frac{\rho}{2}(P_{\text{MG},i}(t) - P_{\text{MG},i}^{k-1}(t))^2\} \end{aligned}$$

s.t.

reformulated $(2)-(12)$ with base-point values $\mathbf{P}_i(t)$,
robust counterpart of Eq.$(5),(7),(8),(10)-(12)$

Step 3: Sub problem for the DC network

$$\begin{aligned} \bar{\mathbf{P}}_{\text{MG},i}^k = &\underset{\bar{P}_{\text{MG},i}(t),P_{ij}(t),l_{ij}(t),v_j(t)}{\text{argmin}} \sum_{t\in\mathcal{T}}\{l_{ij}(t)r_{ij}\\ &+ \sum_{i\in\mathcal{N}}[y_i^k(t)\bar{P}_{\text{MG},i}(t) + \frac{\rho}{2}(\bar{P}_{\text{MG},i}(t) - P_{\text{MG},i}^k(t))^2]\} \end{aligned}$$

s.t.

$$\begin{aligned} &\text{Eq.}(15)-(17)\\ &v_{j,\text{min}} \leq v_j(t) \leq v_{j,\text{max}}, \forall j \in \mathcal{N}, t\in\mathcal{T}\\ &l_{ij}(t) \leq l_{ij,\text{max}}, \forall i\to j \in \mathcal{E}, t\in\mathcal{T} \end{aligned}$$

Step 4: Convergence test
if $\sum_{i\in\mathcal{N}}\sum_{t\in\mathcal{T}}|\bar{P}_{MG,i}^k(t) - P_{MG,i}^k(t)|^2 \leq tol$ **then**
  Return results
else
  $y_i^{k+1}(t) = y_i^k(t) + \rho(\bar{P}_{\text{MG},i}^k(t) - P_{\text{MG},i}^k(t))$
  Go to step 2
end

Algorithm 1: ADMM for problem (28). $\sum_{i\in\mathcal{N}}\sum_{t\in\mathcal{T}}|\bar{P}_{\text{MG},i}^k(t) - P_{\text{MG},i}^k(t)|^2$ is the primal residual. tol is the stopping criteria for ADMM.

the DC network. Once the optimization problem of the DC network is solved and the corresponding auxiliary variables $\bar{P}_{\text{MG},i}(t), \forall i \in \mathcal{N}, t \in \mathcal{T}$ are provided to all the individual MGs. Information is exchanged until convergence .

As can be observed in algorithm 1, each MG only needs update its energy exchange plan with the network to distribution system operator. The distribution system operator shares auxiliary variables to each MGs, together with its corresponding sub-gradient $y_{\text{MG},i}(t), \forall i \in \mathcal{N}, t \in \mathcal{T}$. Detailed models of individual MGs are not required and the distributed algorithm improves efficiency and scalability.

Proposition 1: The above distributed algorithm converges to the global optima in finite steps.

Proof: The APP problem is strictly convex. As shown in algorithm 1, there exits two blocks in ADMM, where one stands for the MGs in step 2 and the other stands for the DC network in step 3. For two block ADMM, recalling the converge proof in Appendix A of [27], this proposition holds.

This article has been accepted for publication in a future issue of this journal, but has not been fully edited. Content may change prior to final publication. Citation information: DOI 10.1109/TSG.2019.2961737, IEEE Transactions on Smart Grid

TABLE I
SYSTEM PARAMETERS

Parameters	MG i 1	2	3
$a_{\text{DG},0,i}$ (\$/kW^2) [30]	0.000132	0.000132	0.000132
$a_{\text{DG},1,i}$ (\$/kW) [30]	0.196	0.1808	0.196
$a_{\text{DG},2,i}$ (\$/kW) [30]	3.548	6.105	3.548
$b_{\text{PV},i}$ (\$/kW) [18]	0.0376	0.0376	0.0376
$c_{\text{ESS,c},i}, c_{\text{ESS,dc},i}$ (\$/kW) [18], [21]	0.108	0.108	0.108
$R_{\text{DG,up},i}, R_{\text{DG,down},i}$ (kW/h)	80	40	40
$P_{\text{DG,max},i}, P_{\text{DG,min},i}$ (kW)	150,10	300,40	150,10
$P_{\text{ESS,max},i}$ (kW)	50	25	25
$E_{\text{ESS,min},i}$ (kWh)	50	50	50
$P_{\text{BIC,max},i}$ (kW)	200	100	100
$P_{\text{UG,max},i}$ (kW)	300	-	-
$\eta_{\text{ESS,c},i}, \eta_{\text{BIC,A2D},i}$	0.95	0.95	0.95
$\eta_{\text{ESS,dc},i}, \eta_{\text{BIC,D2A},i}$	0.90	0.90	0.90

VI. SIMULATION STUDIES

To show the effectiveness the proposed distributed and robust energy management system for networked hybrid AC/DC MGs, two cases are performed in this section. Numerical tests of different scales were carried out on a desktop with an Intel i7-4770 CPU and 128 GB of RAM. The optimization problems are solved by the GUROBI solver [28].

A. Case Description

1) Case I: A system of three networked MGs is simulated to verify the effectiveness of the proposed EMS. MG1 is connected to the UG and three MGs are interconnected to each other via the DC network, as is shown in Fig. 1. The network parameters are extracted from the 4 bus example in [29]. The power capacities of DC transmission lines $l_{1,2}$, $l_{1,3}$ and $l_{2,3}$ are all set at 100kW. The time horizon is 24 hours and time interval is 1 hour. Each MG is equipped with a DG, an ESS, a PV source, a lumped AC load and a lumped DC load. The system parameters are listed in Table I. The profiles of the electricity price, forecast PV output and load demand are referred to [31]. Power capacities of PV arrays in three MGs are set as [100;50;50] kW. The unbalanced power between the forecast load demand and PV generation (i.e. $P_{\text{AC},i}(t) + P_{\text{DC},i}(t) - P_{\text{PV},i}(t)$) for each MG is presented in Fig. 2(a), which should be compensated by the scheduled UG, DG and ESS. The forecast errors for the PV power $\xi^{\max}_{\text{PV},i}$, AC load $\xi^{\max}_{\text{AC},i}$ and DC load $\xi^{\max}_{\text{DC},i}$ are selected as $0.15P_{\text{PV},i}(t)$, $0.05P_{\text{AC},i}(t)$ and $0.05P_{\text{DC},i}(t)$, considering the performance of prevalent forecast algorithms for PV output and loads [32], [33]. The whole sale electricity price is obtained from SDG&E, as shown in Fig. 2(b) [34].

2) Case II: A system of 30 MGs interconnected by a modified IEEE-123 test system is simulated to show the scalability of proposed distributed energy management scheme.

Under both cases, the penalty factor ρ is set at 0.01. The tolerance value in algorithm 1 is set at 10^{-4}. To show the effectiveness and robustness of proposed distributed energy management scheme, the following three scenarios are compared for both cases.

- Scenario I: a centralized deterministic optimization problem is proposed and solved, i.e., problem (1)-(12) with base-point values $\mathbf{P}_i(t)$.

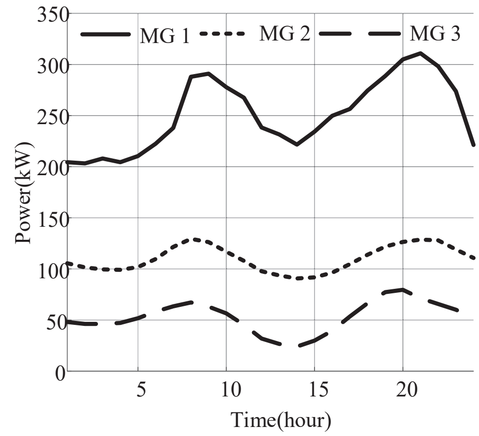

(a)

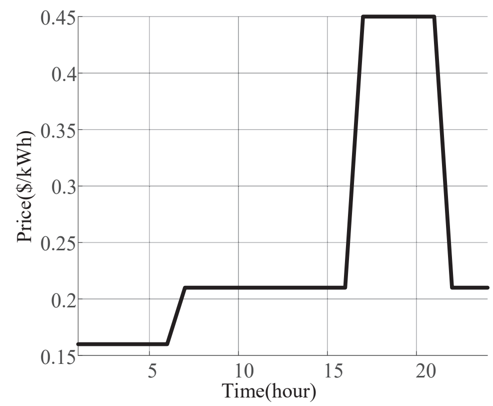

(b)

Fig. 2. The profiles of the forecast power mismatch and the whole electricity price: (a) The unbalanced power between the forecast load demand and PV generation for each MG within the time horizon; (b) The whole sale electricity price within the time horizon [34].

TABLE II
COMPARISON RESULTS UNDER CASE I (A SYSTEM OF THREE NETWORKED MGS)

	Scenario i I	II	III
Objective value(\$)	2,484.84	2,483.89	2,580.33
Running time(s)	0.17	308.14	4.85
Number of decision variables	864	2232	2520
Number of constraints	792	73008	1944

- Scenario II: a centralized stochastic optimization problem is proposed and solved, and the detailed model can be found in Appendix E.
- Scenario III: the proposed distributed and robust optimization problem is solved using algorithm 1.

B. Simulation Results of Case I

1) Computational performance: In Tab.II, the objective functions are revealed under four scenarios, and 100 scenarios

This article has been accepted for publication in a future issue of this journal, but has not been fully edited. Content may change prior to final publication. Citation information: DOI 10.1109/TSG.2019.2961737, IEEE Transactions on Smart Grid

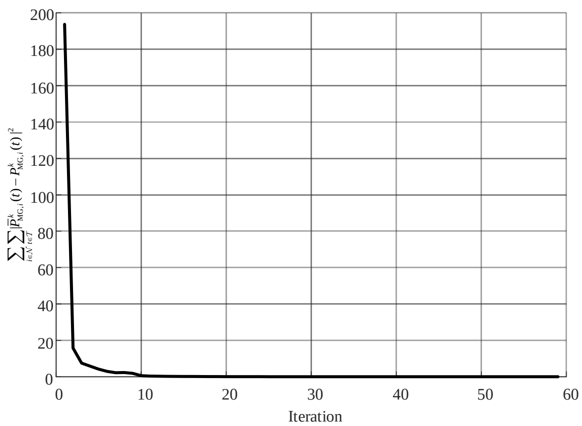

(a)

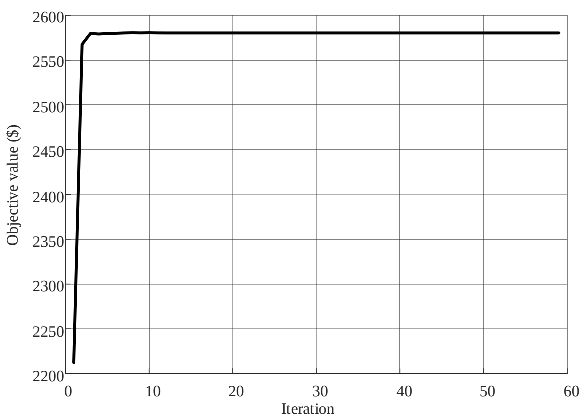

(b)

Fig. 3. Results of iteration process: (a) Convergence curve of primal residuals, i.e., $\sum_{i\in\mathcal{N}}\sum_{t\in\mathcal{T}}|\bar{P}^{k}_{\mathrm{MG},i}(t)-P^{k}_{\mathrm{MG},i}(t)|^2$; (b) Convergence curve of objective value.

are randomly sampled for PV output and load according the uniform distribution under scenario II. As shown in Tab.II, 0.038% difference between the objective value of scenario I and scenario II indicates 100 second stage samples result in provisional objective values between deterministic and stochastic optimization. The minimal cost is obtained under scenario cost with the maximal running time. The objective value of the proposed distributed robust optimization scheme is 3.88% higher than that under scenario II, with 98.42% reduction of running time, as the number of decision variables are reduced by 96.18% and 97.33%, respectively.

The results of the iteration process under scenario III are shown in Fig. 3. It can be observed that, after 59 iterations, the primal residual converges and system optimum value is achieve. In comparison with the stochastic optimization, the proposed distributed robust optimization can reduce the Running time significantly, while increasing the objective values slightly.

2) Scheduling plan: Fig. 4 shows the scheduling results for MG1, MG2 and MG3 under scenario IV, including the power output of the UG, DG, ESS, power transfer from the AC side to the DC side, power exchange from each MG at each hour during a day. During the time period t=8h-20h, the total power output of the UG, DG, ESS in three MGs decreases. This result is coherent with the imbalanced power profile in Fig. 2(a), as the PV systems in three MGs generate power to supply the load demand during this time period. Because only MG1 is connected to the UG, when the electricity price of the UG is lower than the costs of DGs (during the time period t=1h-6h), the UG provides most of the load power in MG1. The output of DG in MG1 goes along with the electricity prices, as shown in Fig.2 b). When the electricity price is low (1h-6h), MG2 and MG3 are absorbing electricity from MG1, and ESS in MG1 is charged. MG2 and MG3 are generating electricity to MG1, and ESS in MG1 is discharged, when the electricity price is high (17h-21h). As can be observed, optimal energy scheduling is achieved with each device operating within its operation constraints; the power sharing among interconnected MGs can improve system efficiency and economy.

Fig. 5 shows results of participation factors for the UG, DG and ESS in three MGs to deal with the forecast error $\xi_i(t)$ within the time horizon. As MG1 is integrated to the UG, the uncertainty is jointly mitigated by the DG, UG and ESS, and the participation factor of the UG is much higher than the other two sources and the UG is the dominant source to supply the load demand. During the time periods t=18h-21h, as the DG is generated at its full capacity in MG3, only ESS is utilized to manage the uncertainty within MG3. Moreover, considering (26), the summation of participation factors is always equal to the unity value, which indicates that the uncertainties (variations of PV and loads) are compensated by the UG, DG and ESS locally within an individual MG and the energy exchange between interconnected MGs becomes a controllable value. This result indicates the effectiveness of the local uncertainty management in the proposed adjustable robust optimization model, which can help to simplify the optimization of the overall system and solve it in a distributed manner with the guaranteed information privacy.

3) Exactness of the relaxation: Simulation results of $\max_{\forall i\in\mathcal{N}}(|P_{\mathrm{ESS,dc},i}(t)P_{\mathrm{ESS,c},i}(t)|)$, $\max_{\forall i\in\mathcal{N}}(|P_{\mathrm{D2A},i}(t)P_{\mathrm{A2D},i}(t)|)$,and $\max_{\forall j\to k\in\mathcal{E}}(|v_j(t)l_{jk}(t)-P^2_{jk}(t)|)$ are shown in Fig. 6. The values are less than 10^{-7}. This verifies the exactness of relaxation in the optimization model in (30) considering network constraints (Lemma 1 and Theorem 1).

4) Robustness of the solutions: To show the robustness of obtained solution, i.e., $\mathbf{P},\beta$, 1000 second stage scenarios are generated, assuming the possibility distribution functions following normal distributions. The outputs of DGs, ESSs and power conversion on BICs are shown in Fig.7, Fig.8 and 9, respectively. Considering the parameters in Tab.I, the power limitations of DGs, ESSs and BICs, i.e., Eq.(5)- (6), Eq.(7)- (8) and Eq.(11)- (12) can be guaranteed. Similar results can be found for the output of UG, indicating the obtained solution can realize the secure operation of the networked MGs.

This article has been accepted for publication in a future issue of this journal, but has not been fully edited. Content may change prior to final publication. Citation information: DOI 10.1109/TSG.2019.2961737, IEEE Transactions on Smart Grid

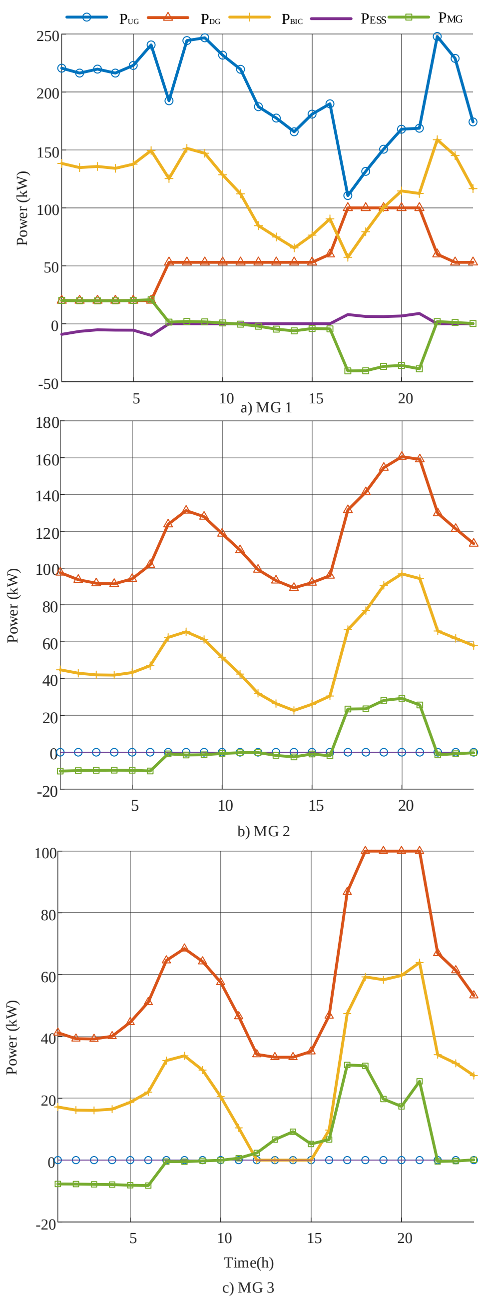

Fig. 4. Scheduling plan among MGs. $P_{\mathrm{BIC}} = P_{\mathrm{BIC,A2D}} - P_{\mathrm{BIC,D2A}}$, $P_{\mathrm{ESS}} = P_{\mathrm{ESS,dc}} - P_{\mathrm{ESS,c}}$

C. Sensitive Analysis of Case I

Fig. 10 shows the sensitivity analysis of system operational cost with regard to different robust levels $\xi_i^{\max}$. The forecast errors of the PV generation, AC load and DC load are set as $\gamma\xi_{\mathrm{PV},i}^{\max}$, $\gamma\xi_{\mathrm{AC},i}^{\max}$ and $\gamma\xi_{\mathrm{DC},i}^{\max}$. As γ increases from 2.5 to 3.5, the operational cost also increase. As the mean value of PV output, AC load and DC load remain the same, the expected operational cost does not change too much along the variation of γ.

The impacts of the interconnection and network constraints are shown in Table III. When the power capacities of three

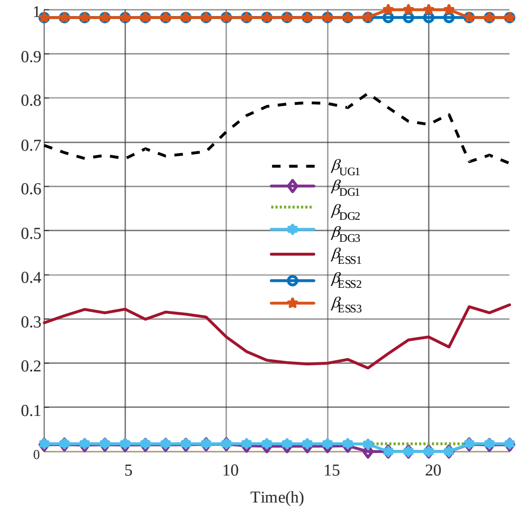

Fig. 5. Participation factors for the UG, DG and ESS in MG1.

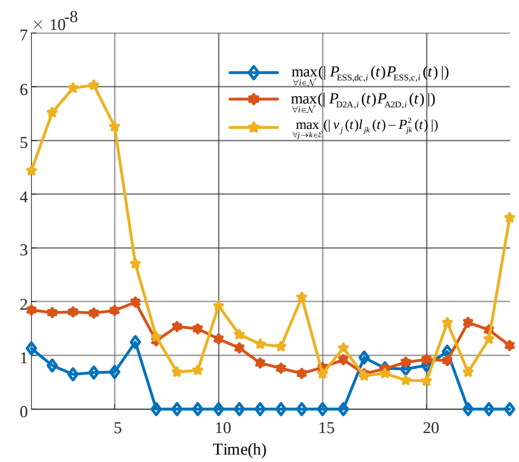

Fig. 6. Verification of Theorem 1

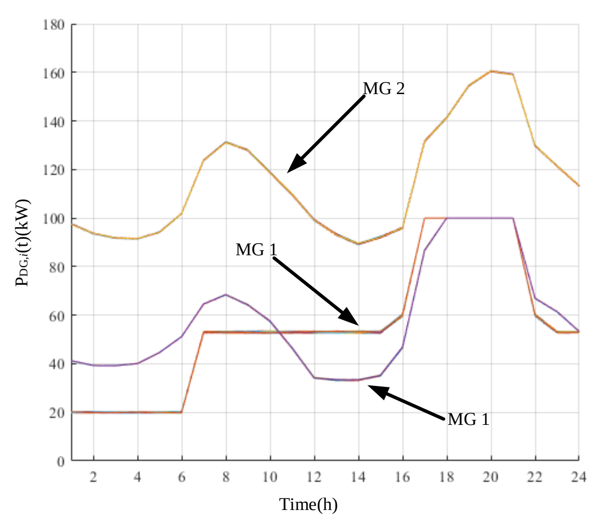

Fig. 7. DG output under 1000 second stage samples

This article has been accepted for publication in a future issue of this journal, but has not been fully edited. Content may change prior to final publication. Citation information: DOI 10.1109/TSG.2019.2961737, IEEE Transactions on Smart Grid

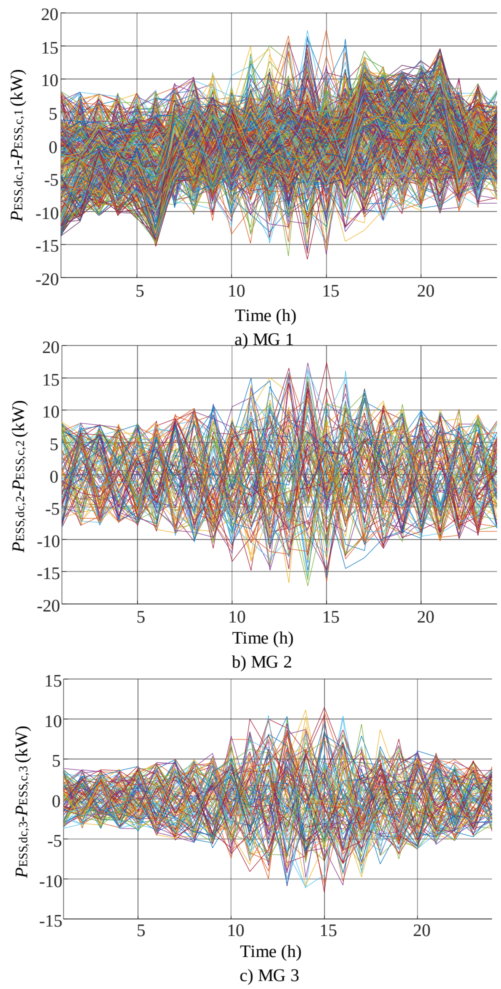

Fig. 8. ESS output under 1000 second stage samples.

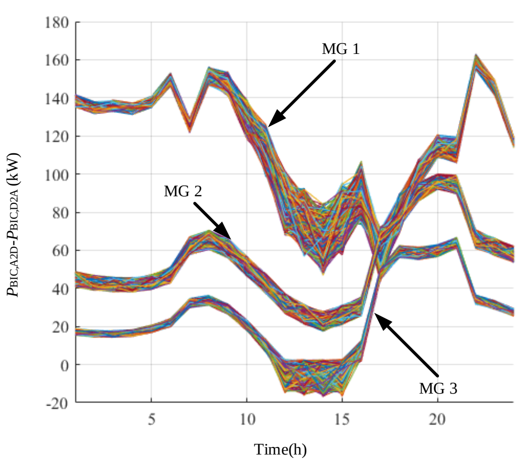

Fig. 9. Power converted on BIC under 1000 second stage samples.

transmission lines are set at 10kW, the operating cost under this situation is 2602.22$, which is larger than the base case (2580.33$) where the transmission line capacities are 100kW. If the MGs operate islandedly without the interconnection (i.e.

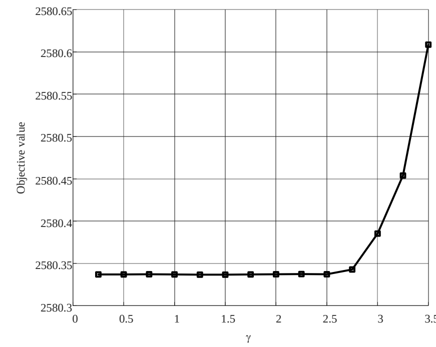

Fig. 10. Operational costs under different robust levels.

TABLE III
IMPACTS OF THE INTERCONNECTION AND NETWORK CONSTRAINTS

Power capacities of transmission lines (kW)			Total operational costs ($)
$l_{1,2}$	$l_{1,3}$	$l_{2,3}$	
100	100	100	2,580.33
10	10	10	2,602.22
0	0	0	2,616.89

the power capacities of three transmission lines are 0), the resulted operational cost of three MGs is 2616.89$. With the interconnection, the total operational cost of the networked MGs reduces and this shows the improved efficiency of the interconnection. The results validate the effectiveness of the optimization model with the network constraints.

D. Simulation Results of Case II

The convergence curve of primal residual and simulation results for case II under three scenarios are given in Fig.11 and Tab.IV, respectively. As shown in Fig.11, with the proposed algorithm, the primal residual converges after 68 iterations, and the optimum value of the large-scale system is achieved at 17,849.24$, which can be observed from Tab.IV. The comparison under the three scenarios in Tab.IV indicates the proposed distributed robust management is comparative with the centralized two-stage stochastic management under scenario II, regarding the objective value and Running time.

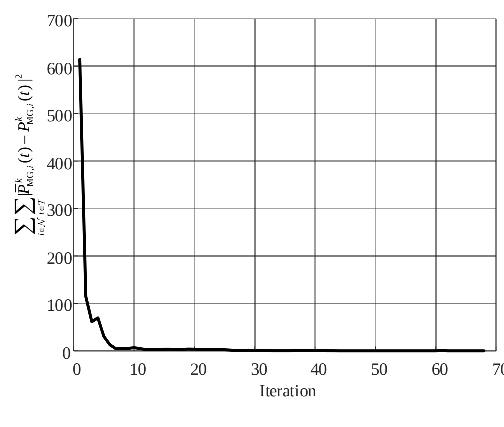

Fig. 11. Convergence curve of primal residuals in case II.

TABLE IV
COMPARISON RESULTS UNDER CASE II(A SYSTEM OF 30 NETWORKED MGS)

	Scenario i I	II	III
Objective value($)	17,849.00	17,840.87	17,849.24
Running time(s)	1.28	471.37	368.92
Number of decision variables	16008	666168	31848
Number of constraints	13800	734520	23880

VII. CONCLUSION

This paper proposes a distributed and robust energy management system for networked hybrid AC/DC MGs. For a single MG, an adjustable robust optimization model is formulated to minimize individual operational cost with the consideration of uncertainties in the renewable generation and load demand. The energy scheduling among interconnected MGs is through the DC network. Then an optimization model of the overall networked-MGs system is constructed to minimize the operational costs and power transmission loss considering physical constraints of the DC network. The optimization model is convectified and solved in a distributed manner by the ADMM algorithm, providing an efficient, reliable, and private-preserving EMS. Case studies are conducted to show the effectiveness of proposed EMS.

APPENDIX A

A. Proof of Lemma 1

Proof: Inspired by the approaches in [35], an optimal solution is assumed to be exited for problem (1)-(12), denoted by $\prod_{t\in\mathcal{T}}\mathbf{p}_i^*(t) := \{p_{\text{UG},i}^*(t), p_{\text{DG},i}^*(t), p_{\text{ESS,c},i}^*(t), p_{\text{ESS,dc},i}^*(t), p_{\text{MG},i}^*(t), p_{\text{D2A},i}^*(t), p_{\text{A2D},i}^*(t), \forall t\in\mathcal{T}\}$, where $p_{\text{ESS,dc},i}(t)p_{\text{ESS,c},i}(t) > 0, \exists t\in\mathcal{T}$ or $p_{\text{A2D},i}(t)p_{\text{D2A},i}(t) > 0, \exists t\in\mathcal{T}$.

The following solution $\prod_{t\in\mathcal{T}}\bar{\mathbf{p}}_i(t) := \{\bar{p}_{\text{UG},i}(t), p_{\text{DG},i}^*(t), \bar{p}_{\text{ESS,c},i}(t), \bar{p}_{\text{ESS,dc},i}(t), \bar{p}_{\text{MG},i}(t), \bar{p}_{\text{D2A},i}(t), \bar{p}_{\text{A2D},i}(t), \forall t\in\mathcal{T}\}$ is formulated in accordance with $\prod_{t\in\mathcal{T}}\mathbf{p}_i^*(t)$, where

$$\bar{p}_{\text{A2D},i}(t) = p_{\text{A2D},i}^*(t) - \varepsilon(t)/2, \forall t\in\mathcal{T}$$

$$\bar{p}_{\text{D2A},i}(t) = p_{\text{D2A},i}^*(t) - \varepsilon(t)/2, \forall t\in\mathcal{T}$$

$$\bar{p}_{\text{UG},i}(t) = p_{\text{UG},i}^*(t) - \varepsilon(t)(1-\eta_{\text{BIC,A2D}})/2, \forall t\in\mathcal{T}$$

$$\bar{p}_{\text{MG},i}(t) = p_{\text{MG},i}^*(t) + \varepsilon(t)(1-\eta_{\text{BIC,D2A}})/2, \forall t\in\mathcal{T}$$

$$\bar{p}_{\text{ESS,dc},i}(t) = \max\{p_{\text{ESS,dc},i}^*(t) - p_{\text{ESS,c},i}^*(t), 0\}, \forall t\in\mathcal{T}$$

$$\bar{p}_{\text{ESS,c},i}(t) = \max\{p_{\text{ESS,c},i}^*(t) - p_{\text{ESS,dc},i}^*(t), 0\}, \forall t\in\mathcal{T}$$

where $\varepsilon(t) = \min\{p_{\text{D2A},i}^*(t), p_{\text{A2D},i}^*(t)\}$, $\varepsilon(t)\geq 0$, $\bar{p}_{\text{ESS,dc},i}(t)\leq p_{\text{ESS,dc},i}(t)$ and $\bar{p}_{\text{ESS,c},i}(t)\leq p_{\text{ESS,c},i}(t)$.

It is clear that, the power balance equations (2) - (3) are met by $\prod_{t\in\mathcal{T}}\bar{\mathbf{p}}_i(t)$. The output of DG is the same in $\prod_{t\in\mathcal{T}}\mathbf{p}_i(t)$ and $\prod_{t\in\mathcal{T}}\bar{\mathbf{p}}_i(t)$, satisfying (5)-(6). The power and energy constraint in (7) - (9) can be met by $\prod_{t\in\mathcal{T}}\bar{\mathbf{p}}_i(t)$ [35]. $\prod_{t\in\mathcal{T}}\bar{\mathbf{p}}_i(t)$ can be easily proved to satisfy the constraints (10)-(12). $\prod_{t\in\mathcal{T}}\bar{\mathbf{p}}_i(t)$ is a feasible solution of problem (1)-(12).

When $p_{\text{ESS,dc},i}(t)p_{\text{ESS,c},i}(t) > 0, \exists t\in\mathcal{T}$ or $p_{\text{A2D},i}(t)p_{\text{D2A},i}(t) > 0, \exists t\in\mathcal{T}$, it is clear that $\sum_{t\in\mathcal{T}} f(\mathbf{p}_i(t)) > \sum_{t\in\mathcal{T}} f(\bar{\mathbf{p}}_i(t))$, as $b_{\text{PV},i} > 0$, $c_{\text{ESS,dc},i} > 0$ and $c_{\text{ESS,c},i} > 0$. It indicates there exits a better solution than $\prod_{t\in\mathcal{T}}\mathbf{p}_i(t)$, contradicting with the problem (1)-(12) is a convex optimization problem, which admits one and only one global optimal solution, as $a_{\text{DG},0,i} > 0$. It finishes the proof.

B. Robust Counterpart of Eq.(5), (7), (8) and (10)-(12)

For the ease of expression, Eq.(5), (7), (8) and (10)-(12) can be formulated as the following compact format:

$$\mathbf{A}_i^{\text{T}}\mathbf{P}_i + \mathbf{B}_i^{\text{T}}\beta_i\xi_i + c_i\xi_i \leq d_i, \forall i\in\mathcal{L} \tag{32}$$

where $\mathcal{L}$ stands for set including Eq.(5), (7), (8) and (10)-(12). ξ_i belongs to the following polyhedron $\mathbf{C}_i\xi_i\leq\mathbf{h}_i$, i.e., Eq.(22).

It should be noted that, in $\mathcal{L}$, Eq.(11)-(12) are replaced by the following equivalent constraints

$$p_{\text{UG},i}(t) + p_{\text{DG},i}(t) - P_{\text{AC},i}(t) + \xi_i(t) \leq P_{\text{BIC,max},i}, \forall t\in\mathcal{T} \tag{33}$$

$$\begin{aligned} &p_{\text{ESS,dc},i}(t) - p_{\text{ESS,c},i}(t) + P_{\text{PV},i}(t) - P_{\text{DC},i}(t) + \\ &\xi_i(t) - p_{\text{MG},i}(t) \leq P_{\text{BIC,max},i}, \forall t\in\mathcal{T} \end{aligned} \tag{34}$$

Using linear duality, the robust counterpart of Eq.(32) is given as follows:

$$\begin{aligned} &\mathbf{A}_i^{\text{T}}\mathbf{P}_i + \mathbf{h}_i^{\text{T}}\mu_i \leq d_i, \forall i\in\mathcal{L} \\ &\mathbf{C}_i^{\text{T}}\mu_i = \beta_i^{\text{T}}\mathbf{B}_i + c_i \\ &\mu_i \geq 0 \end{aligned} \tag{35}$$

C. Proof of Lemma 2

Proof: Firstly, in (30), the upper bound of each bus voltage magnitude is uniform, i.e., the upper bound for each bus is the same,$v_{\max}$. Secondly, there is no limitation on $P_{\text{MG},i}(t)$ in problem (28). Thirdly, for the net injection of each MG, $P_{\text{MG},i}(t)$ is strictly increasing, considering the objective function shown in (27) and power balance conditions shown in Eq.(3). These three conditions satisfy the hypothesis of Theorem 2 in [25]. It finishes the proof.

It should be noted that, Theorem 2 in [25] is for current injection power flow, and the equivalent between the current injection power flow and branch power flow can be found in [36].

D. Proof of Theorem 1

Proof: When the conic relaxation is adopted, problem (31) is a convex QCQP problem, which admits one and only one global optima. Suppose the optimal solution is $\mathbf{x} := \{..., P_{\text{MG},i}^*(t), ...\}, \forall t\in\mathcal{T}$. For given $P_{\text{MG},i}^*(t), \forall t\in\mathcal{T}$, there is no better solution for each MG other than $\mathbf{x}$, which violates constraints (13)-(14), as shown in Lemma 1. In addition, for given $P_{\text{MG},i}^*(t), \forall t\in\mathcal{T}$, there will be no better solution for the DC network other than $\mathbf{x}$, when the upper voltage magnitude limitation for each bus is the same, as shown in Lemma 2. It finishes the proof.

E. Stochastic Optimization Problem under Scenario II

A two-stage stochastic optimization problem is formulated under scenario II, as follows

$$\begin{aligned}
&\min_{\substack{\mathbf{P}_i(t),\mathbf{R}_i(t),\mathbf{p}_{i,\omega}(t),\\ P_{jk}(t),l_{jk}(t),v_j(t)\\ \forall j\in\mathcal{N},j\to k\in\mathcal{E}\\ \forall t\in\mathcal{T},i\in\mathcal{N},\omega\in\Omega}} \mathbb{E}\sum_{t\in\mathcal{T}} f(\mathbf{P}_i(t),\mathbf{R}_i(t),\mathbf{p}_i(t)) = \\
&\sum_{\omega\in\Omega}\sum_{t\in\mathcal{T}} \pi_\omega[a_{\text{DG},0,i}p^2_{\text{DG},i,\omega}(t) + a_{\text{DG},1,i}p_{\text{DG},i,\omega}(t) + \\
&a_{\text{DG},2,i} + b_{\text{PV},i}p_{\text{PV},i,\omega}(t) + \lambda(t)p_{\text{UG},i,\omega}(t) + \\
&c_{\text{ESS,dc},i}p_{\text{ESS,dc},i,\omega}(t) + c_{\text{ESS,c},i}p_{\text{ESS,c},i,\omega}(t)] \\
&\text{s.t.} \\
&P_{\text{DG},i}(t) + R_{\text{DG},i}(t) \le P_{\text{DG,max},i}, \forall t, i \\
&P_{\text{DG,min},i} \le P_{\text{DG},i}(t) - R_{\text{DG},i}(t), \forall t, i \\
&-R_{\text{DG,down},i} \le P_{\text{DG},i}(t) - P_{\text{DG},i}(t-\Delta t) \le R_{\text{DG,up},i}, \forall t, i \\
&P_{\text{UG},i}(t) + R_{\text{UG},i}(t) \le P_{\text{UG,max},i}\forall t, i \\
&0 \le P_{\text{UG},i}(t) - R_{\text{UG},i}(t), \forall t, i \\
&P_{\text{ESS,dc},i}(t) - P_{\text{ESS,c},i}(t) + R_{\text{ESS},i}(t) \le P_{\text{ESS,dc,max},i}, \forall t, i \\
&P_{\text{ESS,c},i}(t) - P_{\text{ESS,dc},i}(t) + R_{\text{ESS},i}(t) \le P_{\text{ESS,c,max},i}, \forall t, i \\
&0 \le P_{\text{ESS,dc},i}(t) \le P_{\text{ESS,dc,max},i}, \forall t, i \\
&0 \le P_{\text{ESS,c},i}(t) \le P_{\text{ESS,c,max},i}, \forall t, i \\
&P_{\text{DG},i}(t) - R_{\text{DG},i}(t) \le p_{\text{DG},i,\omega}(t) \le P_{\text{DG},i}(t) + R_{\text{DG},i}(t), \forall t, i, \omega \\
&P_{\text{UG},i}(t) - R_{\text{UG},i}(t) \le p_{\text{UG},i,\omega}(t) \le P_{\text{UG},i}(t) + R_{\text{UG},i}(t), \forall t, i, \omega \\
&p_{\text{ESS,dc},i,\omega}(t) - p_{\text{ESS,c},i,\omega}(t) \\
&\qquad \le P_{\text{ESS,dc},i}(t) - P_{\text{ESS,c},i}(t) + R_{\text{ESS},i}(t), \forall t, i, \omega \\
&p_{\text{ESS,c},i,\omega}(t) - p_{\text{ESS,dc},i,\omega}(t) \\
&\qquad \le P_{\text{ESS,c},i}(t) - P_{\text{ESS,dc},i}(t) + R_{\text{ESS},i}(t), \forall t, i, \omega \\
&p_{\text{MG},i,\omega}(t) = P_{\text{MG},i}(t), \forall t, i, \omega \\
&\text{Eq.}(2)-(4),(11)-(12)\forall t, i, \omega \\
&\text{Eq.}(15)-(16),(29), \forall t \\
&R_{\text{DG},i}(t) \ge 0, R_{\text{UG},i}(t) \ge 0, R_{\text{ESS},i}(t) \ge 0, \forall t, i
\end{aligned} \tag{36}$$

where $R_{\text{DG},i}(t)$, $R_{\text{UG},i}(t)$ and $R_{\text{ESS},i}(t)$ are the reserve capacity of DG, UG and ESS, respectively. π_ω is the probability of scenario ω.

REFERENCES

[1] S. Parhizi, H. Lotfi, A. Khodaei, and S. Bahramirad, "State of the art in research on microgrids: A review," *IEEE Access*, vol. 3, pp. 890–925, 2015.

[2] N. Hatziargyriou, H. Asano, R. Iravani, and C. Marnay, "Microgrids," *IEEE power and energy magazine*, vol. 5, no. 4, pp. 78–94, 2007.

[3] X. Liu, P. Wang, and P. C. Loh, "A hybrid ac/dc microgrid and its coordination control," *IEEE Transactions on Smart Grid*, vol. 2, no. 2, pp. 278–286, 2011.

[4] A. Gupta, S. Doolla, and K. Chatterjee, "Hybrid ac-dc microgrid: Systematic evaluation of control strategies," *IEEE Transactions on Smart Grid*, 2017.

[5] Q. Xu, J. Xiao, P. Wang, and C. Wen, "A decentralized control strategy for economic operation of autonomous ac, dc, and hybrid ac/dc microgrids," *IEEE Trans. Energy Convers*, vol. 32, no. 4, pp. 1345–1355, 2017.

[6] N. Eghtedarpour and E. Farjah, "Power control and management in a hybrid ac/dc microgrid," *IEEE transactions on smart grid*, vol. 5, no. 3, pp. 1494–1505, 2014.

[7] J. Wu and X. Guan, "Coordinated multi-microgrids optimal control algorithm for smart distribution management system," *IEEE Transactions on Smart Grid*, vol. 4, no. 4, pp. 2174–2181, 2013.

[8] H. Wang and J. Huang, "Incentivizing energy trading for interconnected microgrids," *IEEE Transactions on Smart Grid*, 2016.

[9] P. Tian, X. Xiao, K. Wang, and R. Ding, "A hierarchical energy management system based on hierarchical optimization for microgrid community economic operation," *IEEE Transactions on Smart Grid*, vol. 7, no. 5, pp. 2230–2241, 2016.

[10] M. Marzband, N. Parhizi, M. Savaghebi, and J. M. Guerrero, "Distributed smart decision-making for a multimicrogrid system based on a hierarchical interactive architecture," *IEEE Transactions on Energy Conversion*, vol. 31, no. 2, pp. 637–648, 2016.

[11] Y. Liu, Y. Li, H. B. Gooi, J. Ye, H. Xin, X. Jiang, and J. Pan, "Distributed robust energy management of a multi-microgrid system in the real-time energy market," *IEEE Transactions on Sustainable Energy*, 2017.

[12] T. Lu, Z. Wang, Q. Ai, and W.-J. Lee, "Interactive model for energy management of clustered microgrids," *IEEE Transactions on Industry Applications*, vol. 53, no. 3, pp. 1739–1750, 2017.

[13] Z. Wang, B. Chen, J. Wang, M. M. Begovic, and C. Chen, "Coordinated energy management of networked microgrids in distribution systems," *IEEE Transactions on Smart Grid*, vol. 6, no. 1, pp. 45–53, 2015.

[14] E. Rodriguez-Diaz, E. J. Palacios-Garcia, A. Anvari-Moghaddam, J. C. Vasquez, and J. M. Guerrero, "Real-time energy management system for a hybrid ac/dc residential microgrid," in *2017 IEEE Second International Conference on DC Microgrids (ICDCM)*. IEEE, 2017, pp. 256–261.

[15] P. T. Baboli, M. Shahparasti, M. P. Moghaddam, M. R. Haghifam, and M. Mohamadian, "Energy management and operation modelling of hybrid ac–dc microgrid," *IET Generation, Transmission & Distribution*, vol. 8, no. 10, pp. 1700–1711, 2014.

[16] B. Papari, C. S. Edrington, I. Bhattacharya, and G. Radman, "Effective energy management of hybrid ac–dc microgrids with storage devices," *IEEE transactions on smart grid*, vol. 10, no. 1, pp. 193–203, 2017.

[17] C. Battistelli, Y. P. Agalgaonkar, and B. C. Pal, "Probabilistic dispatch of remote hybrid microgrids including battery storage and load management," *IEEE Transactions on Smart Grid*, vol. 8, no. 3, pp. 1305–1317, 2016.

[18] L. Cost, "Levelized cost and levelized avoided cost of new generation: Resources in the annual energy outlook 2019," *US Energy information administration*, 2019.

[19] M. F. Zia, E. Elbouchikhi, M. Benbouzid, and J. Guerrero, "Energy management system for an islanded microgrid with convex relaxation," *IEEE Transactions on Industry Applications*, 2019.

[20] F. Ueckerdt, L. Hirth, G. Luderer, and O. Edenhofer, "System lcoe: What are the costs of variable renewables?" *Energy*, vol. 63, pp. 61–75, 2013.

[21] Lazard, "Lazard's levelized cost of energy analysis—version 12.0," 2018.

[22] Q. Li and V. Vittal, "Convex hull of the quadratic branch ac power flow equations and its application in radial distribution networks," *IEEE Transactions on Power Systems*, 2017.

[23] G. Keren, N. Cummins, and B. Schuller, "Calibrated prediction intervals for neural network regressors," *IEEE Access*, vol. 6, pp. 54 033–54 041, 2018.

[24] R. A. Jabr, "Adjustable robust opf with renewable energy sources," *IEEE Transactions on Power Systems*, vol. 28, no. 4, pp. 4742–4751, 2013.

[25] L. Gan and S. H. Low, "Optimal power flow in direct current networks," *IEEE Transactions on Power Systems*, vol. 29, no. 6, pp. 2892–2904, 2014.

[26] B. H. Kim and R. Baldick, "A comparison of distributed optimal power flow algorithms," *IEEE Transactions on Power Systems*, vol. 15, no. 2, pp. 599–604, 2000.

[27] S. Boyd, N. Parikh, E. Chu, B. Peleato, and J. Eckstein, "Distributed optimization and statistical learning via the alternating direction method of multipliers," *Foundations and Trends® in Machine Learning*, vol. 3, no. 1, pp. 1–122, 2011.

[28] G. Optimization, "Inc.,"gurobi optimizer reference manual," 2015," 2014.

[29] J. J. Grainger and W. D. Stevenson, *Power system analysis*. McGraw-Hill New York, 1994, vol. 621.

[30] G. Source. Approximate diesel fuel consumption chart. [Online]. Available: https://www.dieselserviceandsupply.com/Diesel_Fuel_Consumption.aspx

[31] Y. Li, T. Zhao, P. Wang, H. B. Gooi, L. Wu, Y. Liu, and J. Ye, "Optimal operation of multimicrogrids via cooperative energy and reserve scheduling," *IEEE Transactions on Industrial Informatics*, vol. 14, no. 8, pp. 3459–3468, 2018.

This article has been accepted for publication in a future issue of this journal, but has not been fully edited. Content may change prior to final publication. Citation information: DOI 10.1109/TSG.2019.2961737, IEEE Transactions on Smart Grid

[32] D. W. Van der Meer, J. Widén, and J. Munkhammar, "Review on probabilistic forecasting of photovoltaic power production and electricity consumption," *Renewable and Sustainable Energy Reviews*, vol. 81, pp. 1484–1512, 2018.

[33] W. Ma, S. Fang, G. Liu, and R. Zhou, "Modeling of district load forecasting for distributed energy system," *Applied Energy*, vol. 204, pp. 181–205, 2017.

[34] R. NikolewskiIi. Time of use rates. [Online]. Available: https://www.sandiegouniontribune.com/business/energy-green/sd-fi-sdge-timeofuse-20190221-story.html

[35] Q. Li and V. Vittal, "Non-iterative enhanced sdp relaxations for optimal scheduling of distributed energy storage in distribution systems," *IEEE Transactions on Power Systems*, vol. 32, no. 3, pp. 1721–1732, 2016.

[36] L. Gan, N. Li, U. Topcu, and S. H. Low, "Exact convex relaxation of optimal power flow in tree networks," *arXiv preprint arXiv:1208.4076*, 2012.

Qianwen Xu (S'14-M'18) received the B.Sc. degree from Tianjin University, China in 2014 and PhD degree from Nanyang Technological University, Singapore in 2018, both in electrical engineering. She has worked as a research associate in Hong Kong Polytechnic University, Hong Kong, and a postdoc research fellow in Aalborg University, Denmark, in 2018. Currently, she is a Wallenberg-NTU Presidential Postdoc Fellow in Nanyang Technological University, Singapore. Her research interests include control, stability, reliability and optimization of microgrids and smart grids.

Tianyang Zhao (S'14'M'18) received the B.E., M.E., and Ph.D. degrees in power systems and its automation from North China Electric Power University, Beijing, China, in 2011, 2013, and 2017, respectively. He is currently a Post-Doctoral Research Fellow with the Energy Research Institute, Nanyang Technological University, Singapore. His research interests include power system operation optimization and game theory.

Yan Xu (S'10-M'13-SM'19) received the B.E. and M.E degrees from South China University of Technology, Guangzhou, China in 2008 and 2011, respectively, and the Ph.D. degree from The University of Newcastle, Australia, in 2013. He is now the Nanyang Assistant Professor at School of Electrical and Electronic Engineering, Nanyang Technological University (NTU), and a Cluster Director at Energy Research Institute @ NTU (ERI@N), Singapore. Previously, he held The University of Sydney Postdoctoral Fellowship in Australia. His research interests include power system stability and control, microgrid, and data-analytics for smart grid applications. Dr Xu is an Editor for IEEE TRANSACTIONS ON SMART GRID, IEEE POWER ENGINEERING LETTERS, CSEE Journal of Power and Energy Systems, and an Associate Editor for IET Generation, Transmission & Distribution.

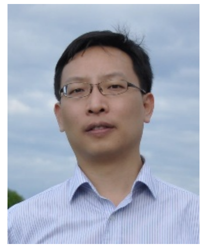

Z hao Xu (M'06-SM'12) received B.Eng, M.Eng and Ph.D degree from Zhejiang University, National University of Singapore, and The University of Queensland in 1996, 2002 and 2006, respectively. From 2006 to 2009, he was an Assistant and later Associate Professor with the Centre for Electric Technology, Technical University of Denmark, Lyngby, Denmark. Since 2010, he has been with The Hong Kong Polytechnic University, where he is currently a Professor in the Department of Electrical Engineering and Leader of Smart Grid Research Area (http://www.mypolyuweb.hk/eezhaoxu/). He is also a foreign Associate Staff of Centre for Electric Technology, Technical University of Denmark. His research interests include demand side, grid integration of wind and solar power, electricity market planning and management, and AI applications. He is an Editor of the Electric Power Components and Systems, the IEEE PES Power Engineering Letter, and the IEEE Transactions on Smart Grid. He is currently the Chairman of IEEE PES/IES/PELS/IAS Joint Chapter in Hong Kong Section.

Peng Wang (M'00- SM'11-F'17) received his B.Sc. degree from Xi'an Jiaotong University, China, in 1978, the M. Sc. degree from Taiyuan University of Technology, China, in 1987, and the M. Sc. and Ph.D. degrees from the University of Saskatchewan, Canada, in 1995 and 1998 respectively. Currently, he is a professor of Nanyang Technological University, Singapore.

Frede Blaabjerg (S'86–M'88–SM'97–F'03) was with ABB-Scandia, Randers, Denmark, from 1987 to 1988. From 1988 to 1992, he got the PhD degree in Electrical Engineering at Aalborg University in 1995. He became an Assistant Professor in 1992, an Associate Professor in 1996, and a Full Professor of power electronics and drives in 1998. From 2017 he became a Villum Investigator. He is honoris causa at University Politehnica Timisoara (UPT), Romania and Tallinn Technical University (TTU) in Estonia.

His current research interests include power electronics and its applications such as in wind turbines, PV systems, reliability, harmonics and adjustable speed drives. He has published more than 600 journal papers in the fields of power electronics and its applications. He is the co-author of four monographs and editor of ten books in power electronics and its applications.

He has received 31 IEEE Prize Paper Awards, the IEEE PELS Distinguished Service Award in 2009, the EPE-PEMC Council Award in 2010, the IEEE William E. Newell Power Electronics Award 2014, the Villum Kann Rasmussen Research Award 2014 and the Global Energy Prize in 2019. He was the Editor-in-Chief of the IEEE TRANSACTIONS ON POWER ELECTRONICS from 2006 to 2012. He has been Distinguished Lecturer for the IEEE Power Electronics Society from 2005 to 2007 and for the IEEE Industry Applications Society from 2010 to 2011 as well as 2017 to 2018. In 2019-2020 he serves a President of IEEE Power Electronics Society. He is Vice-President of the Danish Academy of Technical Sciences too. He is nominated in 2014-2018 by Thomson Reuters to be between the most 250 cited researchers in Engineering in the world.